Available online at www.sciencedirect.com
ScienceDirect
Chaos, Solitons and Fractals 37 (2008) 100–107
CHAOS SOLITONS & FRACTALS
www.elsevier.com/locate/chaos

Non-linear phenomena in electronic systems consisting of coupled single-electron oscillators

Andrew Kilinga Kikombo *, Tetsuya Hirose, Tetsuya Asai, Yoshihito Amemiya

Department of Electrical Engineering, Hokkaido University, Kita 13, Nishi 8, Kita-ku, Sapporo 060-8628, Japan

Accepted 21 August 2007

Abstract

This paper describes non-linear dynamics of electronic systems consisting of single-electron oscillators. A single-electron oscillator is a circuit made up of a tunneling junction and a resistor, and produces simple relaxation oscillation. Coupled with another, single electron oscillators exhibit complex behavior described by a combination of continuous differential equations and discrete difference equations. Computer simulation shows that a double-oscillator system consisting of two coupled oscillators produces multi-periodic oscillation with a single attractor, and that a quadruple-oscillator system consisting of four oscillators also produces multi-periodic oscillation but has a number of possible attractors and takes one of them determined by initial conditions.
© 2007 Elsevier Ltd. All rights reserved.

1. Introduction

The single-electron circuit is an electronic circuit designed to manipulate electronic functions by controlling the transport of individual electrons, making use of the Coulomb blockade phenomenon (Grabert and Devoret [3] have given details). Unlike ordinary electronic circuits, it changes its internal state discontinuously because of electron tunneling and consequently shows complex behavior expressed by a combination of continuous differential equations and discrete difference equations. In this paper, we take up circuit systems consisting of single-electron oscillators and illustrate their non-linear dynamics with the results of computer simulation. A single-electron oscillator is known as the *SET cell* and produces relaxation oscillations with a discontinuous jump in its node voltage. Coupled with one another, single-electron oscillators exhibit high-order non-linear behavior and produce various dynamic phenomena unpredictable from a single oscillator. We found that a double-oscillator circuit consisting of two coupled oscillators produces multi-periodic oscillation with a single attractor. We also found that a quadruple-oscillator circuit consisting of four coupled oscillators has a number of possible attractors and takes one of them determined by the initial value of node voltages – an interesting behavior in dynamical systems (see [4–7] for comprehensive theoretical and numerical study of the long-term behavior of dynamical systems with initial condition dependent attractors of oscillation). The following sections provide details on these studies; we start by making a short sketch of a single oscillator and then describe the behavior of the double- and the quadruple-oscillator systems.

* Corresponding author. Tel.: +81 11 706 7147; fax: +81 11 706 7890.
E-mail address: kikombo@sapiens-ei.eng.hokudai.ac.jp (A.K. Kikombo).

0960-0779/$ - see front matter © 2007 Elsevier Ltd. All rights reserved.
doi:10.1016/j.chaos.2007.08.036

2. Single-electron oscillator

The SET oscillation cell (Fig. 1a) is a constituent element of our single-electron oscillator systems. It consists of a tunneling junction (capacitance $= C_j$) and a high resistance R connected in series at node 1 and biased with a positive or a negative voltage V_d. At low temperatures at which the Coulomb blockade effect is observed (i.e. temperature $\ll e^2/(k_B T C_j)$), the cell produces self-induced relaxation oscillation if $V_d > e/(2C_j)$, where e is the elementary charge and k_B is the Boltzmann constant. See Likharev et al. [1] and Averin et al. [2] for detailed explanation. Fig. 1b shows the waveform of the oscillation of voltage V_1 at node 1 for a positively biased cell. The node voltage gradually increases as junction capacitance C_j is charged through resistance R (curve AB). When the voltage reaches the threshold $e/(2C_j)$, it drops discontinuously to $-e/(2C_j)$ because of an electron tunneling from the ground to node 1 through the junction, again gradually increasing to repeat the same cycles. The dynamics is expressed by a combination of continuous differential equation $dV_1/dt = (V_d - V_1)/(RC_j)$ for charging curve AB and discrete difference equation $\Delta V = -e/C_j$ for discontinuous drop BC, where ΔV is the difference in the node voltage before and after tunneling. The period t_o of oscillation is $t_o = RC_j \ln\left(\frac{V_d + e/2C_j}{V_d - e/2C_j}\right)$ (also see Appendix).

3. Double-oscillator circuit

Coupling positively biased and negatively biased cells (or oscillators) produces interaction between the oscillators and consequently causes complex dynamics of the system. Fig. 2a shows the double-oscillator circuit. The circuit consists of a positively biased oscillator (left) and a negatively biased oscillator (right) coupled through a capacitance C [8]. The variables of this system are node voltages V_1 and V_2. The two oscillators interact with each other through the coupling capacitance: for example, if electron tunneling occurs in the left oscillator from the ground to node 1, then node 1 carries a negative charge to decrease its voltage to a negative, and this induces tunneling in the right oscillator from node 2 to the ground. Because of this interaction, the two oscillators produce synchronization and entrainment. Fig. 2b is a sketch of the dynamics on a V_1–V_2 phase plane. Node voltages V_1 and V_2 change continuously as the junction capacitances are charged through the resistors. When either of the node voltages reaches the threshold, tunneling occurs through the corresponding junction, and this causes a discrete change in both node voltages. For instance, the trajectory of oscillation starts at point 1, proceeds rightward to 2, jumps discontinuously to 3 because of electron tunneling in the left junction, proceeds to 4, jumps to 5 (tunneling in the left junction followed by immediate tunneling in

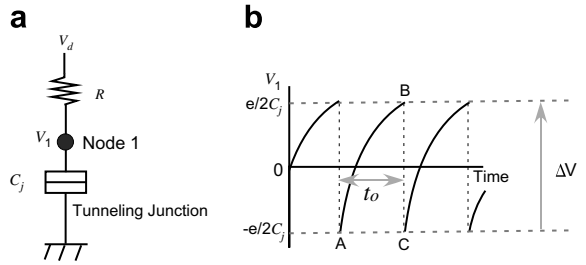

Fig. 1. Single-electron tunneling (SET) cell: (a) circuit configuration and (b) waveform showing oscillation of node voltage V_1.

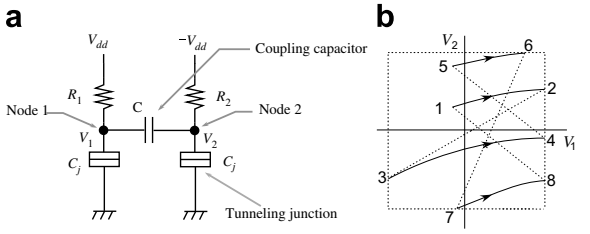

Fig. 2. Double-oscillator circuit: (a) circuit structure consisting of two SET cells coupled through capacitance C and biased with positive and negative voltages V_{dd} and $-V_{dd}$ and (b) sketch showing multi-periodic oscillation in the circuit, plotted on a V_1–V_2 phase plane. Dashed lines show a discrete change caused by tunneling.

the right junction), proceeds to 6, jumps to 7 (tunneling in the right junction), proceeds to 8, and returns to 1 (tunneling in the left junction followed by immediate tunneling in the right junction). This way, the circuit produces a multi-periodic oscillation in which discrete-time and continuous-time dynamics coexist.

To express the dynamics of this circuit, we rewrite the variables and parameters as follows:

$$u_1 = \frac{2C_0}{e}V_1, \quad u_2 = \frac{2C_0}{e}V_2, \quad C_0 = \frac{(2k+1)}{(k+1)}C_j, \quad k = \frac{C}{C_j},$$
$$\alpha = \frac{R_2}{R_1}, \quad \beta = \frac{2C_0}{e}V_{\mathrm{dd}}, \quad \text{and} \quad t = \frac{\text{time}}{R_1 C_0}, \tag{1}$$

where u_1 and u_2 are normalized voltage of nodes 1 and 2, k is the coupling coefficient ($k \geqslant 0$), α is the resistance ratio ($\alpha > 1$), β is the normalized bias voltage ($\beta > 0$), and t is normalized time.

With this rewriting, we can express the dynamics of the system. In a range of $-1 < u_1 < 1$ and $-1 < u_2 < 1$, the system shows continuous-time dynamics (solid curve segments in Fig. 2b) given by differential equations

$$\frac{\mathrm{d}u_1}{\mathrm{d}t} = (\beta - u_1) - \frac{k}{k+1}\frac{1}{\alpha}(\beta + u_2), \tag{2}$$

and

$$\frac{\mathrm{d}u_2}{\mathrm{d}t} = \frac{k}{k+1}(\beta - u_1) - \frac{1}{\alpha}(\beta + u_2). \tag{3}$$

When either of the node voltages u_i exceeds ± 1, electron tunneling occurs, producing a discontinuous jump (dashed lines in Fig. 2b) in node voltages. The differences Δu_1 in node voltage u_1 and Δu_2 in node voltage u_2 before and after tunneling are given by difference equations

$$\Delta u_1 = -2 \quad \text{and} \quad \Delta u_2 = -\frac{2k}{k+1} \tag{4}$$

if u_1 exceeds 1;

$$\Delta u_1 = 2 \quad \text{and} \quad \Delta u_2 = \frac{2k}{k+1} \tag{5}$$

if u_1 falls below -1;

$$\Delta u_1 = -\frac{2k}{k+1} \quad \text{and} \quad \Delta u_2 = -2 \tag{6}$$

if u_2 exceeds 1;

$$\Delta u_1 = \frac{2k}{k+1} \quad \text{and} \quad \Delta u_2 = 2 \tag{7}$$

if u_2 falls below -1.

The double-oscillator circuit produces multi-periodical oscillation with a single attractor on a u_1-u_2 phase plane. We simulated the operation of the circuit for several sets of parameters and plotted the trajectory of the oscillation on a phase plane. The trajectory depended on the initial values of u_1 and u_2 but was attracted, as time passed, to a set of curve segments (i.e., an attractor) independent of the initial values. Fig. 3 shows an example for the circuit with a given set of parameters. In Fig. 3a, oscillation trajectories for two initial states P1 and P2 are depicted. The black curve segments show the transient trajectory originating from initial state P1, and the gray curve segments for initial state P2. The curve segments in Fig. 3b show the attractor to which the trajectories are attracted as time passes. Figs. 4a and b show the attractor for other sets of parameters. A slight change in the coupling coefficient produces a considerable change in the periodicity of oscillation.

The flow of the attractor can be expressed with a sequence of the values of u_2 at which the attractor meets line $u_1 = 1$. For example, the attractor shown in Fig. 3b can be expressed with a sequence of 3 values of u_2, and attractors in Figs. 4a and b can be expressed with 55 and 11 values of u_2, respectively. The number of these u_2 values is the degree of periodicity in oscillation. To take a general view of the effect of the coupling coefficient on the degree of periodicity, we drew a bifurcation diagram that plotted the set of the u_2 values as a function of k. Fig. 5 shows the diagram, simulated with $\beta = 3$ and $\alpha = \sqrt{10}$. At $k = 0$, the two oscillators in the circuit produced a self-induced oscillation independent of each other. As k increased, the oscillators began to interact with each other to produce synchronized periodic oscillation. Generally speaking, the degree of periodicity increased with the increase of k. However, windows (or regions in which the degree of periodicity drops) appeared repeatedly.

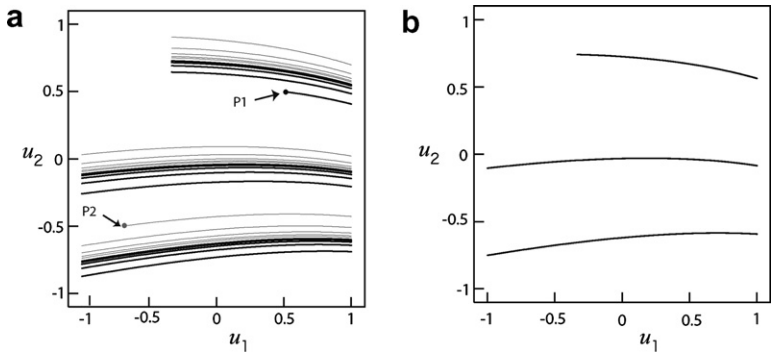

Fig. 3. Attractor of the double-oscillator circuit, simulated with coupling coefficient $k = 0.5$, resistance ratio $\alpha = \sqrt{10}$, and bias voltage $\beta = 3$. (a) Trajectories starting from two initial states P1 = (0.5,0.5) and P2 = (−0.7, −0.5) (black curve segments for P1, gray curve segments for P2), and (b) attractor that the trajectories settle down to.

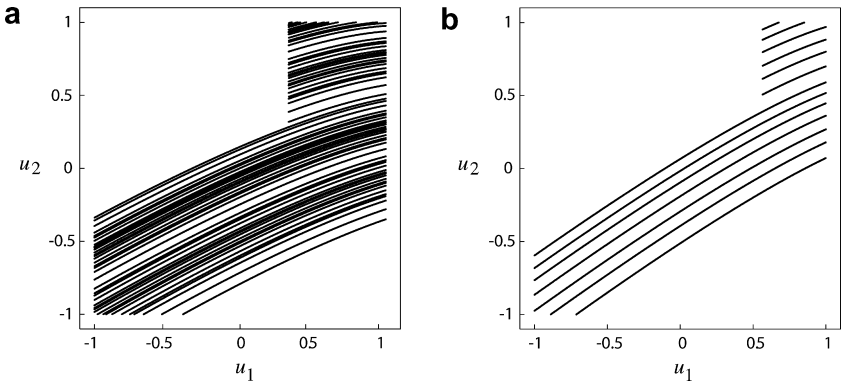

Fig. 4. Two examples of the attractor simulated with (a) $k = 2$ and (b) $k = 3.6$, with $\alpha = \sqrt{10}$ and $\beta = 3$ for both figures.

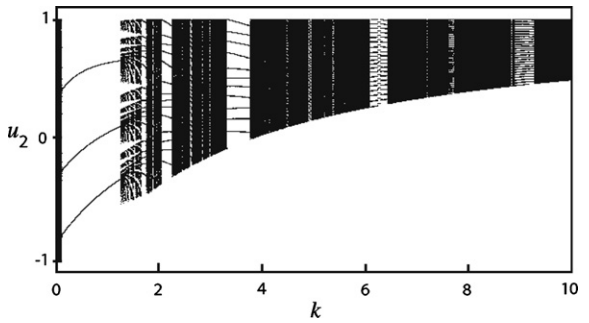

Fig. 5. Bifurcation diagram with k as a bifurcation parameter, with $\alpha = \sqrt{10}$ and $\beta = 3$.

4. Quadruple-oscillator circuit

Coupling two double-oscillator circuits will produce a new system with more complex dynamics. Fig. 6 shows such a quadruple-oscillator system consisting of four oscillators – two are positively biased with V_{dd} and the other two are negatively biased with $-V_{dd}$. The oscillators are connected in a ring through coupling capacitors C so that electron tunneling in one oscillator will induce tunneling in the two adjacent oscillators. The variables of this system are four node voltages V_1, V_2, V_3, and V_4.

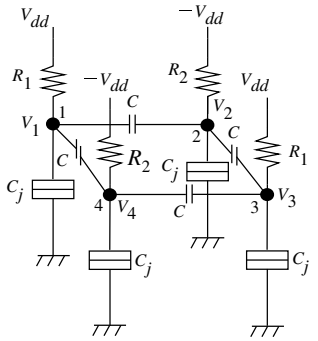

Fig. 6. Quadruple-oscillator circuit consisting of two double-oscillator circuits coupled through capacitors C.

To express the dynamics of this circuit, we rewrite the variables and parameters as

$$\begin{aligned} &u_i = \frac{2C_s V_i}{e} \quad (i = 1-4), \quad C_s = \frac{(8k^2+6k+1)C_j}{(2k^2+4k+1)}, \\ &k = \frac{C}{C_j}, \quad \alpha = \frac{R_2}{R_1}, \quad \beta = \frac{2C_s}{e}V_{\mathrm{dd}}, \quad \text{and} \quad t = \frac{\text{time}}{R_1 C_s}, \end{aligned} \tag{8}$$

where u_i is the normalized voltage of the ith node, k is the coupling coefficient ($k \geqslant 0$), α is the resistance ratio ($\alpha > 1$), β is the normalized bias voltage ($\beta > 0$), and t is normalized time.

With this rewriting, we calculated the dynamics of the system. In a range of $-1 < u_i < 1$ ($i = 1$–4), the system dynamics are given by differential equations

$$\begin{aligned} \frac{\mathrm{d}u_1}{\mathrm{d}t} &= -\frac{2(\gamma+\zeta-\kappa-\eta)k^2 + (-4\kappa+\gamma+\zeta)k - \kappa}{(4k+1)(2k+1)} \\ \frac{\mathrm{d}u_2}{\mathrm{d}t} &= -\frac{2(\gamma+\zeta-\kappa-\eta)k^2 + (4\gamma-\kappa-\eta)k + \gamma}{(4k+1)(2k+1)} \\ \frac{\mathrm{d}u_3}{\mathrm{d}t} &= -\frac{2(\gamma+\zeta-\kappa-\eta)k^2 + (-4\eta+\zeta+\gamma)k - \eta}{(4k+1)(2k+1)} \\ \frac{\mathrm{d}u_4}{\mathrm{d}t} &= -\frac{2(\gamma+\zeta-\kappa-\eta)k^2 + (4\zeta-\kappa-\eta)k + \zeta}{(4k+1)(2k+1)}, \end{aligned} \tag{9}$$

where

$$\begin{aligned} &\gamma = \frac{\beta+u_2}{\alpha}, \quad \zeta = \frac{\beta+u_4}{\alpha}, \\ &\kappa = \beta - u_1, \quad \eta = \beta - u_3. \end{aligned} \tag{10}$$

When any of node voltages u_i reaches the threshold value of ± 1, an electron tunnels at the corresponding node, and this leads to a discrete change in node voltages of the four nodes of the system. For instance, if u_1 reaches $+1$, tunneling occurs in oscillator 1 from the ground to node 1. This produces a discontinuous change in node voltage given by difference equations

$$\Delta u_1 = -2 \tag{11}$$

for node 1,

$$\Delta u_2 \quad \text{and} \quad \Delta u_4 = -\frac{2k(2k+1)}{2k^2+4k+1} \tag{12}$$

for the two adjacent nodes 2 and 4, and

$$\Delta u_3 = -\frac{4k^2}{2k^2+4k+1} \tag{13}$$

for the diagonally positioned node 3. In case u_1 falls below -1, electron tunnels from node 1 to the ground, and the change is positive for every node voltage. Tunneling at any other node leads to a similar change in the four node voltages.

We simulated the operation of the quadruple-oscillator circuit for various parameter settings and found that this system showed multi-periodic oscillation with a number of possible attractors instead of a single attractor. The attractor the system actually took was determined by the initial values of the four node voltages u_i ($i = 1$–4); in other words, some initial conditions evolve to a certain attractor, and other initial conditions evolve to a different attractor. To understand the behavior of this system entirely, we need to draw four-dimensional basin diagrams for various parameter settings. However, drawing such basin diagrams requires a long numerical computer simulation. We are currently carrying out computer simulations on the basin diagram but have yet to complete it. Therefore, we will show only part of our simulation still in progress.

Fig. 7 shows an example, a simplified two-dimensional basin diagram for a sample parameter setting of $k = 1$, $\alpha = \sqrt{10}$, and $\beta = 3$. It was drawn as follows:

(step 1): The attractor of oscillation was calculated and plotted on a four-dimensional u_1–u_2–u_3–u_4 phase space for a given initial condition (u_{01}, u_{02}, u_{03}, u_{04}), where u_{0i} are the initial values of node voltages u_i. For simplicity, the initial voltages of nodes 1 and 3 (and initial voltages of nodes 2 and 4) were assumed to be the same in amplitude but inverse in polarity: i.e., $u_{03} = -u_{01}$ and $u_{04} = -u_{02}$. Therefore initial conditions can be plotted on an u_1–u_2 plane.

(step 2): The calculated attractor was orthogonally projected onto the u_1–u_2 plane to reduce its dimensions. The projected attractor consisted of a number of curve segments on the u_1–u_2 plane. Figs. 7a and b show the projected attractor for two sample initial conditions.

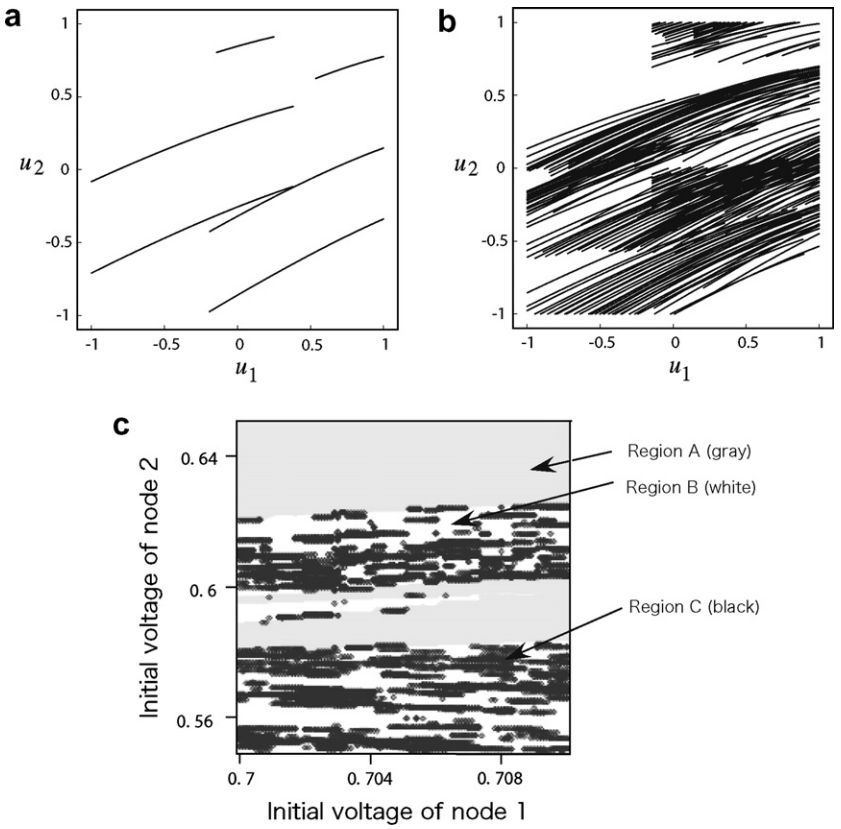

Fig. 7. Attractors and basins of the quadruple-oscillator circuit, simulated with a parameter setting of $k = 1$, $\alpha = \sqrt{10}$ and $\beta = 3$. (a,b) two of the three attractors projected onto a u_1–u_2 plane, and (c) basin for the attractors. Regions A, B, and C are the attracting basins for the first (a), the second (b) and the third attractors, respectively.

(step 3): Steps 1, 2 and 3 were repeated many times to obtain projected attractors for various initial conditions.
(step 4): The basins of attraction for the projected attractors were depicted on a u_1–u_2 plane.

The resultant basin diagram is Fig. 7c. The sample system has three possible attractors; the first is shown by Fig. 7a, the second is shown by Fig. 7b, and the third is similar to Fig. 7b but the number of curve segments is somewhat smaller. The attractor actually taken was determined by the initial conditions: that is, initial conditions in region A in Fig. 7c

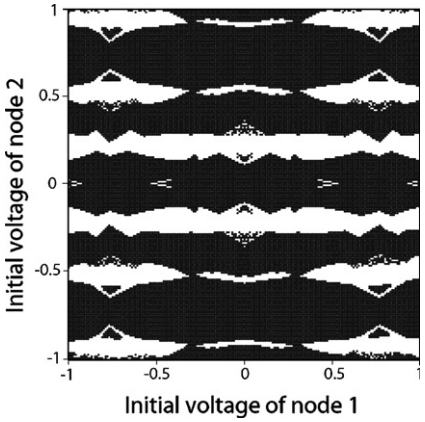

Fig. 8. The whole of the basin diagram for a parameter setting of $k = 1$, $\alpha = \sqrt{10}$ and $\beta = 3$. Shaded regions are the basins of the first attractor (Fig. 7a), and non-shaded regions are the basins of the second (Fig. 7b) and the third attractors.

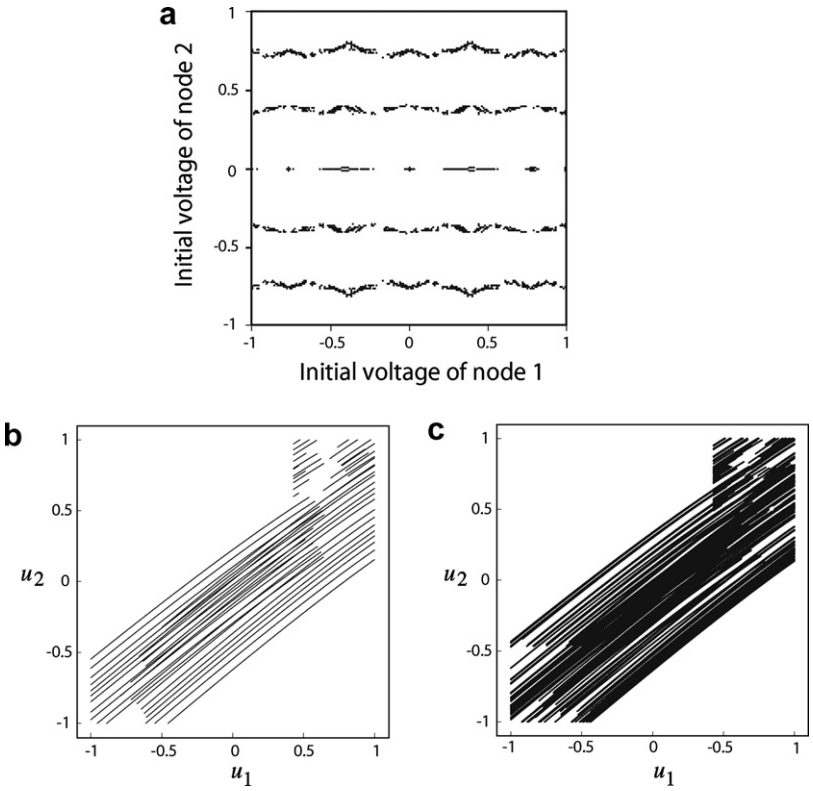

Fig. 9. Basin diagram (a) for a parameter setting of $k = 3.6$, $\alpha = \sqrt{10}$, and $\beta = 3$. Three possible attractors exist. Shaded regions in (a) are the basin of one attractor (b) and non-shaded regions are the basins of the other two attractors (one is shown in (c)).

lead to the first attractor (Fig. 7a), initial conditions in region B lead to the second attractor (Fig. 7b), and initial conditions in region C lead to the third attractor.

Fig. 8 shows the whole of the basin diagram on a u_1–u_2 plane ($-1 < u_1 < 1$ and $-1 < u_2 < 1$). The shaded regions are the basins of the first attractor (Fig. 7a), and non-shaded regions are the basins of the second and the third attractors (these two are labyrinthine and undistinguishable on the figure).

Fig. 9 shows another example, calculated with a parameter setting of $k = 3.6$, $\alpha = \sqrt{10}$, and $\beta = 3$. Also three possible attractors exist. The shaded regions in Fig. 9a are the basins of one attractor (Fig. 9b) and non-shaded regions are the basins of the other two attractors (one is shown in Fig. 9c).

5. Summary

Coupled single-electron oscillators are electronic complex systems whose dynamics is described by a combination of continuous differential equations and discrete difference equations. Computer simulation shows that the complexity of system's operation increases as the number of coupled oscillators increase. That is, (i) a single oscillator shows only simple relaxation oscillation, (ii) the double-oscillator system produces multi-periodic oscillation with a single attractor, and (iii) the quadruple-oscillator system also produces multi-periodic oscillation but has a number of possible attractors and takes one of them, as determined by the initial conditions. An open question is what kind of complexity would appear in systems with larger number of coupled oscillators. For example, what kind of new complexity would appear in a double quadruple-oscillator system? To answer this, we are now analysing and simulating the operation of large-scale coupled oscillator systems.

Appendix. Waiting time for tunneling

Strictly speaking, tunneling is a stochastic process with a probabilistic delay between when the node voltage exceeds threshold voltage $e/(2C_j)$ and when actual tunneling event takes place. Therefore, the period of oscillation shows probabilistic fluctuation expressed by $t_o+\Delta t$, where probabilistic delay or waiting time Δt varies at every tunneling event. However, we have theoretically confirmed that waiting time decreases to a value far smaller than t_o as resistance R increases. We can consider normalized waiting time to be 0 if we use a sufficiently large resistance. The situation is the same in the circuits described in Sections 3 and 4.

References

[1] Likharev KK, Zorin AB. J Low Temp Phys 1985;59:347–82.
[2] Averin DV, Likharev KK. J Low Temp Phys 1986;62:345–73.
[3] Grabert H, Devoret MH. Single charge tunneling. New York: Plenum Press; 1992.
[4] Xiao-Song Y. Chaos, Solitons & Fractals 2002;15:655–7.
[5] Bezruchko BP, Prokhorov MD, Seleznev YeP. Chaos, Solitons & Fractals 2003;15:695–711.
[6] Xiao-Song Y. Chaos, Solitons & Fractals 2003;16:147–50.
[7] Feudel U, Grebogi C, Poon L, Yorke JA. Chaos, Solitons & Fractals 1998;9:171–80.
[8] Kikombo AK, Oya T, Asai T, Amemiya Y. In: Proceedings of 13th international workshop on non-linear dynamics of electronic systems, Potsdam, Germany 2005.